Shape resonances in modified effective-range theory for electron-molecule collisions

Zbigniew Idziaszek

Instytut Fizyki Teoretycznej, Uniwersytet Warszawski, 00-681 Warszawa, Poland and
Centrum Fizyki Teoretycznej, Polska Akademia Nauk, 02-668 Warszawa, Poland

Grzegorz Karwasz

Instytut Fizyki, Uniwersytet Mikołaja Kopernika, 87-100 Toruń, Poland

We develop a simple model of shape resonances in electron-molecule collisions that is based on the modified effective-range expansion and analytical solutions of the Schrödinger equation for the long-range part of the interaction potential. We apply our model to electron scattering on N_2 and CO_2. The parameters of the effective-range expansion (i.e. the scattering length and the effective range) are determined from experimental, integral elastic cross sections in the 0.1 - 1.0 eV energy range. For both molecular targets our treatment predicts shape resonances that appear slightly higher than experimentally known resonances in total cross sections. Agreement with the experiment can be improved by assuming the position of the resonance in a given partial wave. Influence of quadrupole potential on resonances is also discussed: it can be disregarded for N_2 but gets significant for CO_2. In conclusion, our model developed within the effective range formalism reproduces well both the very low-energy behavior of the integral cross section as well as the presence of resonances in the few eV range.

I. INTRODUCTION

$^2\Pi$ temporary negative ion states in N_2 and CO_2 at 2.1 eV and 3.8 eV [1, 2] respectively, are the best known examples of so-called shape resonances, in which the incoming electron is captured within the potential well of the target, rather than to a specific electronic orbital. This distinction came clearly from the first discovery of the shape (in N_2) and Feshbach (in He [3]) resonances by Schulz, see detailed discussion in Ref. [4, 5].

The widths and amplitudes of these resonances, as appearing in total cross sections, are well established, see for ex. Ref. [6, 7, 8] for N_2 and [9, 10] for CO_2. In both resonances the vibrational excitation contributes significantly to the total cross section (about 1/6 in N_2 and 1/3 in CO_2, see [11]); both targets are non-polar, with negligible direct rotational excitation cross sections.

However, apart from the resonances, the low-energy dependences of total cross section in N_2 and CO_2 differ completely: the cross section rises sharply in the zero-energy limit in CO_2 [12] and falls slowly in N_2 [7]. Particularly, the CO_2 scattering received a rich theoretical treatment, starting from the early assignment of this state as shape $^2\Pi_u$ state [13] and calculations using model potentials, for ex. by Morrison and co-workers [14, 15, 16]. More recent works, both experimental [17] and theoretical [18], indicate that the mechanism of this resonance is complex, with coupling between different vibrational modes; the analysis requires the vibrational excitations to be included [19]. However, with few exceptions [14, 20] calculations were performed separately for the zero-energy and resonance energy ranges, see for ex. [16, 19, 21, 22, 23, 24].

In our previous work [25] we revisited a rather old problem - application of the modified effective range theory (MERT) to electron and positron scattering [26]. In that theory the scattering is due to the polarization potential and the short range potential is modelled by an effective range expansion. These features make MERT particularly suitable for the near-to-zero energy range, treated with difficulties in other approaches [27, 28]. The near-to-zero energy MERT expansion continues to be applied to numerous problems: integral cross sections for atoms [29, 30], non-polar [31, 32] and polar molecules [33, 34]. MERT is frequently used by experimentalists for extrapolation of measured differential and integral cross sections towards energies and angles inaccessible by experiment [35, 36, 37]. Different extensions of MERT, consisting in developing phase shifts (or elements of the reactance, K matrix) into series of k were applied by Morrison et al. [27] to rotational excitation of N_2 molecule, and by Macri and Barrachina to electron - metastable He scattering and electron photodetachment from Li^- [38, 39].

The most extensive, to our knowledge, analysis of MERT applicability in electron scattering was done for noble gases by Buckman and Mitroy [40]. They concluded that MERT fails above about 1 eV, exact energy depending on the target. However, in that as well in numerous other MERT applications, those were integral cross sections which were developed directly in series of the colliding electron momentum k. As we showed in the previous work [25], the range of applicability of such a series is limited to a few tenths of eV. Therein [25] we proposed a novel way of applying MERT. It consists in calculating the phase shifts due to the polarization potential from Mathieus solutions of the Schrödinger equation and introducing the effective-range expansion *exlusively for the short-range potential*. There is no explicit k expansion for the integral cross sections in our approach; only the short-range contribution expressed in terms of

an appropriate boundary condition, is expressed as series of k. This makes the numerical procedures more complicated but allows to extend the applicability of MERT for positron-argon and -nitrogen scattering to the range of 2-3 eV. We note that our method closely resembles quantum-defect-theory formulation of the scattering problem, where the quantum-defect parameter, that slowly varies with energy, is expanded in a series of k (see e.g. [41]). In electron-atom scattering the quantum-defect theory has been already applied by Watanabe and Greene [42] to analyze photodetachment process of K^- and by Fabrikant [43] to low-energy electron-metal atoms resonances.

In this paper we apply our MERT-based model to the two molecules N_2 and CO_2, well studied by beam and swarm techniques at energies down to less than 0.1 eV. The parameters of MERT expansion for the short-range potential are derived from fitting procedure using the recommended [44] integral cross sections below 1 eV. Next, we use these potentials to calculate cross sections up to 10 eV. In both molecules broad p-wave resonances appear. In such an unconstrained fit the resonances appear at higher energies than experimental values. By small, within the experimental error bar, modifications of the data used for the inversion procedure, one can reproduce the exact position of the resonances. In that case both resonances appearing in the p or d-partial wave channels are narrower than experimentally determined (but this can be partially caused by neglecting the nuclear motion, see for ex. Ref. [19]). We discuss also the relative contributions to integral cross sections from the non-spherical part of the polarizability and the quadrupole moment of molecule, using the distorted-wave approximation.

The paper is organized as follows. In section II we discuss the analytical solutions of the Schrödinger equation with the polarization potentials, and we present principles of the modified effective-range expansion. In section III we demonstrate that MERT accounts for shape resonances in p and d waves, assuming some simplified model of electron-molecule potential. The actual electron resonances in N_2 and CO_2 are analyzed in section IV. Section V discusses correction to MERT cross sections due to the non-spherical part of the polarization potential and the molecule quadrupole moment. We present some conclusions in section VI. Finally, three appendices give some technical details of the analytical solutions for the polarization potential.

II. SCATTERING OF A CHARGED PARTICLE ON A MOLECULE AND THE QUANTUM-DEFECT APPROACH

The relative motion of a charged particle and a nonpolar molecule is described by the Schrödinger equation

$$\left[-\frac{\hbar^2}{2\mu}\Delta + V(\mathbf{r}) - E \right] \Psi(\mathbf{r}) = 0, \qquad (1)$$

where μ is the reduced mass, E is the relative energy of the particles, and $V(\mathbf{r})$ is the particle-molecule potential. $V(\mathbf{r})$ can be written as a sum

$$V(\mathbf{r}) = V_1(\mathbf{r}) + V_2(\mathbf{r}) + V_S(r) \qquad (2)$$

of long-range contributions

$$V_1(\mathbf{r}) = -\frac{\alpha e^2}{2r^4} \qquad (3)$$

$$V_2(\mathbf{r}) = -\left(\frac{\alpha_2 e^2}{2r^4} + \frac{Q}{r^3} \right) P_2(\cos\theta) \qquad (4)$$

and a short-range potential $V_S(r)$. The long-range potential is expressed in terms of the static spherical and non-spherical polarizabilities α and α_2, respectively, and the quadrupole moment Q. The short-range part $V_S(r)$ comes into play at the distances comparable to the size of the molecule, where the molecule cannot be treated as a single object. Numerous approaches were proposed in the past, based on modifications of the polarization potential [45], deriving the short-range interaction from electronic densities etc. [46], or expanding the scattering amplitude at low energies [43]. In the present approach we express $V_S(r)$ in terms of some boundary conditions imposed on the wave function at $r \to 0$, while the effects resulting from the finite range of $V_s(r)$ are included explicitly in the framework of the modified effective-range theory.

In the following we assume that the nonisotropic part $V_2(\mathbf{r})$ can be neglected in comparison to the isotropic polarization potential $V_1(\mathbf{r})$. This is justified as long as the quadrupole moment Q and the nonspherical polarizability α_2 expressed in atomic units are much smaller than α_0. In such a case the main effect of the nonisotropic terms is the coupling between different partial waves, while their contribution to the total cross-section at low energies remains small. As we show later in section Sec. V, where we analyze the corrections arising from $V_2(\mathbf{r})$, this is a good approximation for N_2 and CO_2 molecules. The MERT analysis for these molecules is performed in Sec. IV.

The radial part of the Schrödinger equation with the isotropic polarization potential $V_1(\mathbf{r})$ reads

$$\left[\frac{\partial^2}{\partial r^2} - \frac{l(l+1)}{r^2} + \frac{(R^*)^2}{r^4} + \frac{2\mu E}{\hbar^2} \right] \Psi_l(r) = 0, \quad (5)$$

where $\Psi_l(r)$ denotes the radial wave function for the partial wave l. For the polarization potential, it is convenient to introduce some characteristic units R^* and E^*, where $R^* \equiv \sqrt{\alpha e^2 \mu/\hbar^2}$ denotes the characteristic length of the r^{-4} potential, and $E^* = \hbar^2/(2\mu R^{*2})$ is the characteristic energy. With appropriate change of variables, the Schrödinger equation (5) can be transformed into Mathieu's differential equation of the imaginary argument [26, 47, 48], and solved analytically in terms of the continued fractions. Some basic properties of the analytical solutions are discussed in Appendices A, B, and

C (see [49, 50] for more details on Mathieu functions). Here, we focus only on the behavior at small and large distances. For $r \ll R^*$, when the polarization potential dominates over centrifugal potential and the constant energy term, behavior of $\Psi_l(r)$ is given by

$$\Psi_l(r) \overset{r \to 0}{\sim} r \sin\left(\frac{R^*}{r} + \phi_l\right), \qquad (6)$$

where ϕ_l is a short-range phase, which is determined by $V_s(r)$. For $E = 0$ and $l = 0$ the solution (6) becomes exact at all distances, and from its asymptotic behavior at large distances one can easily determine the value of the s-wave scattering length

$$a_s = -R^* \cot(\phi_0). \qquad (7)$$

At large distances: $r \gg R^*$, $\Psi_l(r)$ must take the form of the scattered wave

$$\Psi_l(r) \overset{r \to \infty}{\sim} \sin(kr - l\tfrac{\pi}{2} + \eta_l), \qquad (8)$$

where $k = \sqrt{2\mu E}/\hbar$. Using the Mathieu functions one can find the following relation between the phase shift η_l and the short range phase ϕ_l [26]

$$\tan \eta_l = \frac{m^2 - \tan \delta^2 + \tan(\phi_l + l\frac{\pi}{2}) \tan \delta (m^2 - 1)}{\tan \delta (1 - m^2) + \tan(\phi_l + l\frac{\pi}{2})(1 - m^2 \tan^2 \delta)}, \qquad (9)$$

where $\delta = \frac{\pi}{2}(\nu - l - \frac{1}{2})$, and m and ν are some parameters, that are determined by the analytical solutions (see Appendices A and B for details).

In general, the parameter ϕ_l entering the asymptotic formula (6), depends on energy, and can be expanded in powers of k. In our case it is more convenient to expand $\tan(\phi_l + l\frac{\pi}{2})$, entering formula (9):

$$\tan(\phi_l + l\tfrac{\pi}{2}) = A_l + \frac{1}{2}R^* R_l k^2 + \ldots, \qquad (10)$$

where $A_l \equiv \tan(\phi_l + l\frac{\pi}{2})\big|_{q=0}$. The lowest order correction in k is quadratic, and can be interpreted as an effective range R_l for the partial wave l [26].

Combining (9), (10), (C1), (C2) one can easily obtain the low-energy expansion of the phase shifts [26]

$$q \cot \eta_0 = -\frac{1}{a} + \frac{\pi}{3a^2}q + \frac{4}{3a}\ln\left(\frac{q}{4}\right)q^2 + \frac{R_0{}^2}{2}q^2$$
$$+ \left[\frac{\pi}{3} + \frac{20}{9a} - \frac{\pi}{3a^2} - \frac{\pi^2}{9a^3} - \frac{8}{3a}\psi(\tfrac{3}{2})\right]q^2 + \ldots \qquad (11)$$

$$\tan \eta_l = \frac{\pi q^2}{8(l - \frac{1}{2})(l + \frac{1}{2})(l + \frac{3}{2})} + \ldots, \quad l \geq 1 \qquad (12)$$

Here, $q = kR^*$, $a = a_s/R^* = -1/A_0$, and $b = A_1$. The low-energy expansions (11)-(12) are applicable only at small energies $E \ll e^*$. In contrast, in our approach we use the exact formula (9) for the phase shift, with the short-range phase expanded according to (10).
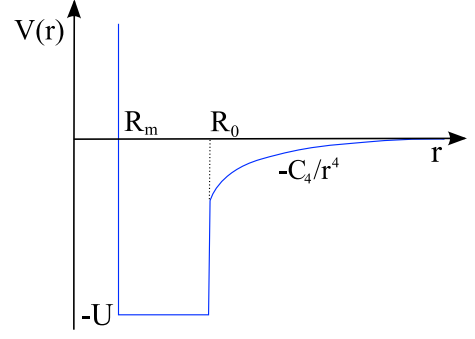

FIG. 1: The model potential Eq.(13) that is used to test MERT for the shape resonances

III. MODEL CALCULATION

To illustrate how MERT describes shape resonances for the long-range r^{-4} potential we consider a simple model of the potential with a square-well interaction at short distances (see Fig.1)

$$V(r) = \begin{cases} \infty & r < R_m \\ -U & R_m < r < R_0 \\ -C_4/r^4 & r > R_0 \end{cases} \qquad (13)$$

Here, R_m denotes a hard-core radius and R_0 is the radius of the square-well potential. The potential $V(r)$ does not reproduce the full behavior of the electron-molecule interaction, however, it captures the basic properties of shape resonances in such a system, and allows to verify the accuracy of our MERT-based approach. The Schrödinger equation for the potential $V(r)$ and partial-wave quantum number l can be solved exactly:

$$\Psi(r) = \begin{cases} 0, & r < R_m \\ rj_l(\chi r) + Cry_l(\chi r), & R_m < r < R_0 \\ A\sqrt{r}M_\nu\left(\ln\frac{\sqrt{R^*}}{\sqrt{kr}}\right) + B\sqrt{r}T_\nu\left(\ln\frac{\sqrt{R^*}}{\sqrt{kr}}\right), & r > R_0 \end{cases} \qquad (14)$$

where $\hbar^2\chi^2/(2\mu) = E + U$ and constants A, B, C are to be determined from the continuity conditions for $\Psi(r)$ at $r = R_m$ and $r = R_0$. With the help of the asymptotic formulas (B3) and (B4) for $M_\nu(z)$ and $T_\nu(z)$ for large and negative arguments (large r) we find the phase shifts and the total cross-section for scattering on $V(r)$. We compare the exact results with our MERT model where the MERT coefficients A_l and R_l are found by expanding the formula $\tan(\phi_l + \nu\frac{\pi}{2} + \frac{\pi}{4}) = A/B$ (c.f. Eq. (B6)) in the powers of q, and utilizing series expansion (C1) for the characteristic exponent.

Fig. 2 shows the dependence of the total elastic cross-section on energy, for few particular values of U, for which p-wave shape-resonances appear. The range R_0 was chosen to be smaller than R^*, but still, of the same order as R^*, that roughly corresponds to the conditions of the low-energy electron(positron)-molecule scattering. The resonances show up as peaks at some particular values
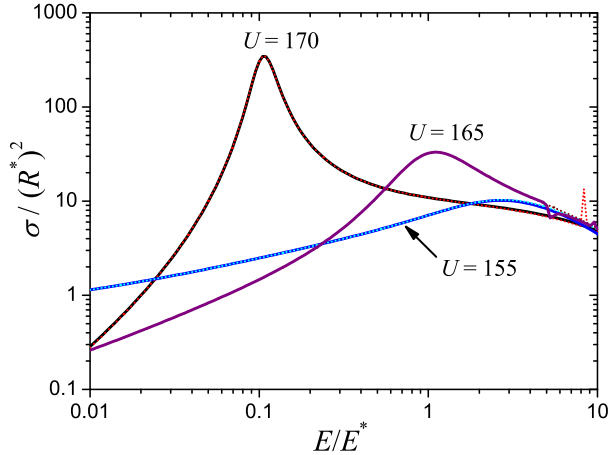
FIG. 2: Total elastic cross-section versus energy for the scattering in the model potential (13), calculated for $R_m = 0.1R^*$, $R_0 = 0.5R^*$ and for different depths U of the square-well potential. Results are scaled by the the characteristic distance R^* and the characteristic energy E^* of the polarization potential. The peaks correspond to the p-wave shape resonances, that are accurately reproduced by MERT.

FIG. 3: Same as Fig. 2, but for values of U for which shape resonances in d wave appear.

of the energy. We observe that MERT, including only two lowest expansion coefficients A_l and R_l of the short-range potential, reproduces very accurately the exact results. The accuracy decreases for higher energies, where one can observe some discrepancies, in particular small peaks corresponding to the g-wave resonances that appear at different energies for exact and MERT curves. This results from higher sensitivity of the quasi-bound states on the parameters of the short-range potential for larger l, and the absence of the higher order terms in expansion (10) when E becomes too large. Nevertheless, the approximate MERT treatment remains very accurate for the main resonances in p-wave channel, even for energies significantly larger than E^*.

A similar comparison, but for d-wave resonances is presented in Fig. 3. In this case the resonance peaks are narrower due to the stronger centrifugal barrier, and weaker coupling between quasi-bound and scattering states. Again, the agreement between MERT and the exact results is very good, and some discrepancies can be observed only at $E \sim 10E^*$. Finally, we note that for $l = 2$ and parameters of Fig. 3 the quasi-bound state is totally localized within the range of the short-range potential. This shows that MERT is able to reproduce shape resonances resulting solely from the short-range potential, even if the latter is treated in terms of an effective-range expansion.
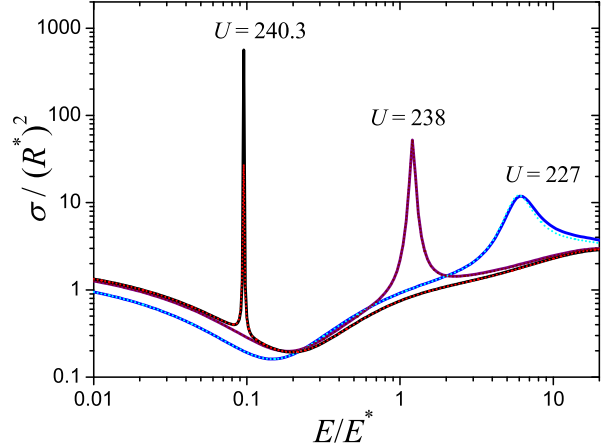
IV.   MERT ANALYSIS OF LOW-ENERGY ELECTRON SCATTERING

We investigate the low-energy electron scattering on N_2 and CO_2 molecules using a theoretical model based on MERT for s and p partial waves [25]. Our model contains four unknown parameters: the scattering length $a = a_s/R^* = -1/A_0$ and the effective range R_0 for s wave, and the zero-energy contribution A_1 and the effective range R_1 for p wave, that are determined by fitting to the experimental data. In this way for $l = 0$ and $l = 1$ we neglect corrections of the order higher than q^2 in expansion (10). On the other hand, for partial waves with $l \geq 2$ we include only the lowest-order contribution to the scattering phase shifts that are due to the long-range polarization potential (12). This is sufficient as long as the energy E remains smaller than the centrifugal barrier, that for $l = 2$ has height of $9E^*$. The total elastic cross-section $\sigma(k) = 4\pi k^{-2} \sum_l \sin^2 \eta_l(k)$ is determined from the phase shifts (9) and (12), with ν and m evaluated numerically, using the procedure described in Appendices A and B.

In the calculations we use recent experimental values of the polarizability, as measured in electron scattering experiments: $\alpha = 11.54 a_0^3$ for N_2 and $\alpha = 16.92 a_0^3$ for CO_2 [51]. First, we fit our model by the least-square, not weighted method to the experimental data exclusively below the resonances, i.e. for energies $E \leq 1.2$eV and $E \leq 2$eV for N_2 and CO_2, respectively, down to the lowest energies available from beam experiments [44]. The fitted parameters from this check are listed in Table I. Note, that the scattering potential parameters are expressed in characteristic distance units. For example, in N_2 the scattering length a_s amounts to 0.404 atomic units, close to the value of 0.420 a.u. derived by Morrison et al. [27]. Subsequently, we extend MERT analysis,
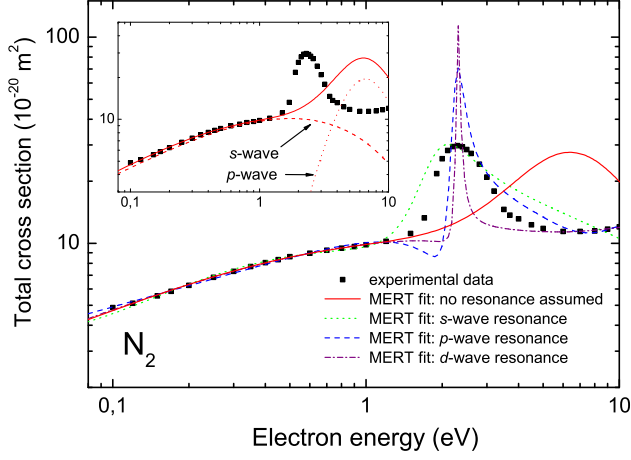
FIG. 4: Total cross-section for the scattering of electrons on N_2 versus the energy. Depicted are: recommended experimental data from review [44] (stars), the theoretical fits based on MERT, assuming the resonance at 2.1eV in s wave (dotted line), p wave (dashed line), and d wave (dot-dashed line), and without assumption with respect to the position of the resonance (solid line). The inset shows in addition the s-wave and p-wave contributions to the MERT fit not assuming the position of resonance.
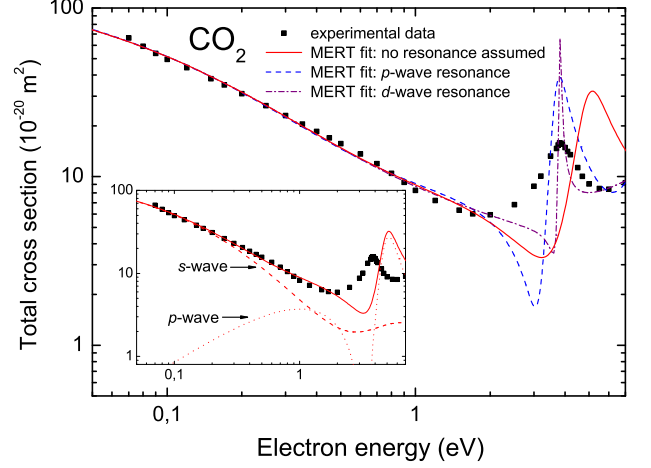

FIG. 5: The same as fig. 4 but for the scattering of electrons on CO_2 with the recommended experimental data from review [44]. Note, missing curve corresponding to s-wave resonance, which does not fit well to the experimental data in this case.

	$R^*(a_0)$	E^*(eV)	a	A_1	R_0/R^*	R_1/R^*
N_2	3.397	1.179	0.119	-0.537	0.110	0.262
CO_2	4.113	0.8041	-1.606	-3.537	-0.325	1.208

TABLE I: Characteristic distance R^*, characteristic energy E^* and four fitting parameters: $a = a_s/R^*$ (s-wave scattering length), A_1 (zero-energy contribution from the short-range potentials for p-wave), R_0 (s-wave effective range), and R_1 (p-wave effective range) for N_2 and CO_2 in the case of unconstrained fits and using only the very low energy experimental data.

using the fitted parameters to higher energies. Figs. 4 and 5 compare the experimental data (points) with the theoretical curves obtained from this fit (solid lines). For both molecules resonance maxima appear in the scattering cross-section, however they are located at somewhat higher energies that the experimental ones (about 6 eV for N_2 and 5 eV for CO_2). For both molecules these "spontaneously" appearing resonances are due to the p-wave, see inserts in Fig. 4 and 5. In the case of CO_2 the p-wave is subject to rapid changes also below the resonance. This is to be attributed to large values of b and R_1 of the potential (see table I). Note that in experiment [52] some vibrational modes (001) show resonant maxima below the main 3.6 eV peak.

The range of fitted data corresponds to quite low energies in terms of characteristic units: $E \lesssim E^*$ ($E \lesssim 2.5E^*$) for N_2 (CO_2). Therefore, the fitting procedure, within the error bar of experimental points, is not able to pre-

dict with sufficient accuracy the cross section in the energy range corresponding to resonance peaks. Also, neglection of the nonisotropic part of the potential leads to some additional errors. Moreover, our scheme neglects the possibility of d-wave or higher partial wave resonances, that can be suggested e.g. by the behavior of differential cross-section for the scattering on N_2. To eliminate these shortcomings we have subsequently added to the fitting procedure also some experimental points, located in the energy range above the resonance: $6eV < E < 10eV$ (N_2), and $5.5eV < E < 7eV$ (CO_2). In addition we have considered three possible scenario assuming that resonances occur in partial waves s, p or d, exactly at the energy of the resonance peak observed in the experimental data. This corresponds to the requirement that the phase shift η_l assumes value $\pi/2$ at the peak location for $l = 0, 1, 2$, respectively. In this way we obtain some constrains on the six fitting parameters: a, A_1, A_2 (zero-energy contributions) and R_0, R_1 and R_2 (effective ranges). The results are shown in Figs. 4 and 5, presenting apart from the previous data, also theoretical curves with resonances assumed in s, p and d waves. The fitted parameters are listed in tables II and III.

We observe that for N_2 the height of the resonance peak for s wave agrees well with the experimental data (we show experimental values averaged over the vibrational structure seen in the resonance, following recommended data from ref. [44]). This would suggest a possible s-wave origin of the resonance. But this point requires some more detailed discussion.

As said before, the generally accepted classification of resonances describes "shape" resonances as occurring within the shape of the effective potential, formed from the static and polarization contributions with the centrifugal barrier added. Obviously, for the s-wave the cen-

	a	A_1	A_2	R_0/R^*	R_1/R^*	R_2/R^*
s-wave res.	-0.447	-0.021	—	-3.100	-0.104	—
p-wave res.	0.157	-4.314	-0.130	-47.05	4.704	0.079
d-wave res.	0.123	-0.390	-0.222	-0.301	-0.174	0.293

TABLE II: Six fitting parameters: $a = a_s/R^*$ (s-wave scattering length), A_1 (zero-energy contribution for p-wave), A_2 (zero-energy contribution for d-wave), R_0 (s-wave effective range), R_1 (p-wave effective range) and R_2 (d-wave effective range) for N_2 in the case of fits assuming shape resonances in s, p and d waves. The fits are made to the data below and above the resonance (see text for details). Note that for s-wave resonance only four parameters (two partial waves) were sufficient to fit the data.

	a	A_1	A_2	R_0/R^*	R_1/R^*	R_2/R^*
p-wave res.	-1.616	-6.250	-0.406	-0.266	2.780	0.131
d-wave res.	-1.605	-2.470	-2.624	-0.340	-0.234	1.180

TABLE III: Six fitting parameters: $a = a_s/R^*$ (s-wave scattering length), A_1 (zero-energy contribution for p-wave), A_2 (zero-energy contribution for d-wave), R_0 (s-wave effective range), R_1 (p-wave effective range) and R_2 (d-wave effective range) for CO_2 in the case of fits assuming shape resonances in p and d waves. The fits are made to the data below and above the resonance (see text for details).

trifugal barrier does not exist so trapping of the electron within the shape of the effective potential is impossible. However, our calculations show a quick change in the s-wave phase shift, occurring approximately in the region of the experimentally observed resonance so following the interpretation by Fano [53, 54] we would classify this state as a resonance. On the other hand, assumption of resonances in p and d waves would lead to much narrower and higher peaks in the total cross section than the experimental values. Therefore, a simple interpretation of the the N_2 resonance is not easy: i) elastic differential cross sections at the resonance maximum (2.47 eV) show a dominating p-wave contribution, ii) differential cross sections for the first vibrational excitation (ν=0-1) at 2.45 eV show almost a perfect d-wave dependence [52] while iii) the MERT analysis does not exclude the resonance in the s-partial wave. Clearly, several partial waves contribute to the resonance and MERT analysis is not able to separate these contributions.

For CO_2 the MERT fit with constraints does not improve much the agreement with the experimental total cross sections, see Fig. 3. The MERT analysis excludes completely the s-wave resonance, and both p and d wave resonances differ much in amplitude and width from the experimental values. For CO_2 resonance the interplay of different partial waves is even more complex than for N_2. On the other hand, recent calculations [18, 20] and experiments [17] showed that the broad peak in CO_2 cross section is rather a superposition of two resonances for dif-

ferent molecular geometries, resulting from the bent configuration in the dominating vibrationally excited mode (010).

V. CORRECTIONS DUE TO THE NONISOTROPIC PART OF THE LONG-RANGE POTENTIAL

Already early works stressed importance of other, apart from the sperical polarization, components of the long-range potential. For both molecules the non-sperical part of the polarizability is rather strong (see table IV); for CO_2 also the quadrupole moment is significant. In the present analysis we approximate the quadrupole and non-spherical polarizability contributions together, but using two distinct methods for the zero-energy limit and at low $E \sim E^*$ energies. To analyze the contribution from the nonisotropic part of the potential at very low energies ($E \ll E^*$), we can compare the small-k series expansions for the whole potential $V_1(r) + V_2(r)$ [56], to the expansion including the spherical part $V_1(r)$ only. For the isotropic part, the total cross-section for scattering on N_2 and CO_2 molecules can be obtained from expansions of the phase shifts given by Eqs. (11)-(12). Substituting the parameters of the potential listed in the Table IV one obtains

$$\frac{\sigma_{N_2}(q)}{4\pi} = a^2 + 24.60qa + 31.32q^2 \log(q)a^2 + O(q^3) \tag{15}$$

$$\frac{\sigma_{CO_2}(q)}{4\pi} = a^2 + 35.44qa + 45.12q^2 \log(q)a^2 + O(q^3) \tag{16}$$

$$\tag{17}$$

On the other hand, application of the small-k expansion for the full potential [56] leads to

$$\frac{\sigma_{N_2}(q)}{4\pi} = a^2 + 24.93qa + 0.23q + 0.11$$
$$+ 31.63(a - 0.15)(a + 0.16)q^2 \log(q) + O(q^3) \tag{18}$$

$$\frac{\sigma_{CO_2}(q)}{4\pi} = a^2 + 39.56qa - 3.97q + 1.32$$
$$+ 49.09(a - 0.53)(a + 0.56)q^2 \log(q) + O(q^3) \tag{19}$$

We observe that for the typical scales of the scattering length $a \sim 1$, the differences in the coefficients of Eqs.(18)-(19) and Eqs.(15)-(16) are at most of the order of 10%.

For higher energies $E \sim E^*$ the importance of the nonisotropic part can be assessed with the help of the distorted wave approximation [57]. The scattering amplitude can be written as a sum of the contributions from

	$\alpha(a_0^3)$	$\alpha_2(a_0^3)$	$Q(ea_0^2)$
N_2	11.54	3.08	-1.09
CO_2	16.92	9.20	-3.86

TABLE IV: Parameters of the long-range potential $V_L(\mathbf{r})$ for molecules considered in our analysis. For α_0 we use recent experimental values of [51], and for α_2 and Q we use experimental values used in Refs. [27] for N_2 and in Ref. [14] for CO_2

.

V_1 and V_2 separately (see e.g. [58])

$$f(\mathbf{k}_f, \mathbf{k}_i) = -\frac{m}{2\pi\hbar^2} \left(\langle \mathbf{k}_f | V_1 | \Phi^+(\mathbf{k}_i) \rangle + \langle \Phi^-(\mathbf{k}_f) | V_2 | \Psi^+ \rangle \right), \tag{20}$$

where $\Phi^\pm(\mathbf{k})$ is the scattering state for the isotropic part V_1

$$\Phi^\pm(\mathbf{k}) = e^{i\mathbf{k}\mathbf{r}} + G_0^\pm V_1 \Phi^\pm(\mathbf{k}), \tag{21}$$

$G_0^\pm$ is the free propagator

$$G_0^\pm = \lim_{\epsilon \to 0} (E - \mathbf{p}^2/2m \pm i\epsilon)^{-1}, \tag{22}$$

and Ψ^+ is the scattering state for the full potential, satisfying the the following Lippmann-Schwinger equation

$$\Psi^+ = \Phi^+(\mathbf{k}_i) + G_1^+ V_2 \Psi^+, \tag{23}$$

$$G_1^+ = \lim_{\epsilon \to 0} (E - \mathbf{p}^2/2m - V_1 + i\epsilon)^{-1}. \tag{24}$$

The second term in Eq. (20) can be written in the form of a Born series

$$\langle \Phi^-(\mathbf{k}_f) | V_2 | \Psi^+ \rangle = \langle \Phi^-(\mathbf{k}_f) | V_2 + V_2 G_1^+ V_2 + \ldots | \Phi^+(\mathbf{k}_i) \rangle. \tag{25}$$

Finally, the total cross-section can be calculated applying the optical theorem $\sigma = \frac{4\pi}{k} \text{Im} f(\mathbf{k}_i, \mathbf{k}_i)$.

After averaging over different orientations of molecules, the lowest order contribution from the nonisotropic part of the potential $\langle \Phi^-(\mathbf{k}_f) | V_2 | \Phi^+(\mathbf{k}_i) \rangle$ vanishes, and for small anisotropic part, the leading contribution is provided by $\langle \Phi^-(\mathbf{k}_f) | V_2 G_1^+ V_2 | \Phi^+(\mathbf{k}_i) \rangle$. We evaluate this term using analytical solutions for the spherical potential V_1 and introducing an additional cut-off parameter R_0, that describes the distance when the interaction potential takes a form of the long range potential $V_1 + V_2$, which is roughly of the order of the size of the molecule.

Tables V and VI list the the corrections due to the nonisotropic part V_2, together with total cross sections coming from the isotropic part V_1. The analytical unperturbed solution for V_1 was calculated for parameters of Table (I), corresponding to the low-energy fits. For N_2 the corrections are small, of the order of 1%. On the other hand, for CO_2, the corrections are as large as 40% of the total cross-section σ_0, therefore in this case an accurate analysis would require full inclusion of V_2. We note that corrections slightly depend on the cut-off

E/E^*	σ_0	$R_0 = 0.5R^*$	$R_0 = 0.75R^*$	$R_0 = R^*$
1.0	3.145	0.0306	0.0311	0.0300
2.0	4.014	0.0147	0.0135	0.0138
4.0	7.428	0.0059	0.0052	0.0053

TABLE V: The total elastic cross-section σ_0 and corrections due to the nonspherical part of the long-range potential in N_2 molecule, for different energies E of the scattered electron and different short-range cut-off parameters R_0.

E/E^*	σ_0	$R_0 = 0.5R^*$	$R_0 = 0.75R^*$	$R_0 = R^*$
1.0	2.185	0.174	0.796	0.698
2.0	1.345	0.455	0.514	0.363
4.0	0.693	0.207	0.213	0.153

TABLE VI: The total elastic cross-section σ_0 and corrections due to the nonspherical part of the long-range potential in CO_2 molecule, for different energies E of the scattered electron and different short-range cut-off parameters R_0.

parameter R_0, that is a consequence of the fact that the analytical solutions for the purely polarization potential V_1 are not physical at small distances, where the short-range part of the potential comes into play. Therefore corrections listed in tables V and VI estimate contributions of V_2 from large distances only, where the potential takes the asymptotic form $V_1 + V_2$.

VI. CONCLUSIONS

MERT analytical solution was applied previously [25] for positron scattering cross sections. Those cross sections fall monotonically with energy, up to the positronium formation threshold, and do not exhibit particular structures, see [59]. The model approximated well Ar and N_2 integral elastic cross sections at 0-2 eV. The derived scattering potentials were characterized by negative values of the scattering length-like parameters: a and A_1, for s and p waves, respectively.

At present, the MERT analysis was applied for electron scattering on non-polar molecules, N_2 and CO_2. Parameters of the short range potential (the scattering length and the effective range) for the s, p, and for higher energies also the d partial wave, were fitted. The model approximates very well the experimental data up to about 1-2 eV. The s-wave scattering length deduced is positive for N_2 and negative for CO_2. Deriving the potential parameters from the experimental data below resonance and using them again for our model at higher energies, we obtained p-wave resonances for both molecules, although at slightly higher energies than observed experimentally. To check for the consistency of the fit, the model was applied jointly to the data below and above resonance, assuming that the resonance occur the in s, p or d wave,

at the energy as observed experimentally. Within the latter constraint, for N_2 a "resonance-like" peak, corresponding to the $\pi/2$ phase change appears also in the s-wave channel. In that case the peak is not as sharp as pure shape resonances in p and d partial waves.

As far as amplitude are considered, in N_2 fixing the resonance position reproduces well the absolute value of the total cross section in its maximum, but only if the resonance is assumed to appear in the s-wave channel. Such a fixed fit does not improve the agreement in the case of CO_2. More experimental points at low energies, also for N_2, would be useful for such a modelling. By the way, we recall that Ramanan and Freeman [60], on the basis of their swarm experiment even stated: "experimental data presently available do not rule out the existence of a Ramsauer-Townsend minimum at an electron energy of 0.4 meV or lower".

Summarizing, the present work unifies in a single model the very low-energy dependence of the integral cross sections in N_2 and CO_2 with the occurrence of shape resonances at a few eV energies. It confirms that limitations on applicability of MERT to the very low energy range, come rather from direct expansions of the phase-shifts in series of k, rather than from any intrinsic defects of the effective range model. Obviously, several aspects of resonant scattering, like partitioning between the elastic and vibrational/rotational excitation are beyond the capacities of our model. It would be challenging to incorporate MERT potentials to more advanced theoretical treatments, in particular of inelastic direct and resonant scattering [19, 20, 21].

APPENDIX A: SOLUTIONS OF THE SCHRÖDINGER EQUATION FOR $1/r^4$ POTENTIAL

The method for solving the Schrödinger equation with the polarization potential was discussed in our previous paper [25]. Below we indicate the basic steps of the derivation. In the radial Schrödinger equation (5) we substitute $r = \sqrt{R^*}e^{-z}/\sqrt{k}$ and $\Psi_l(r) = \psi(r)\sqrt{r/R^*}$, which yields the Mathieu's modified differential equation [49, 50]

$$\frac{d^2\psi}{dz^2} - [a - 2q\cosh 2z]\,\psi = 0. \qquad (A1)$$

where $a = (l + \frac{1}{2})^2$ and $q = kR^*$. Two linearly independent solutions $M(z)$ and $T(z)$ can be expressed in the

following form [48, 49]

$$M_\nu(z) = \sum_{n=-\infty}^{\infty} (-1)^n c_n(\nu) J_{2n+\nu}(2\sqrt{q}\cosh z), \; (A2)$$

$$T_\nu(z) = \sum_{n=-\infty}^{\infty} (-1)^n c_n(\nu) Y_{2n+\nu}(2\sqrt{q}\cosh z), \; (A3)$$

Here, ν denotes the characteristic exponent, and $J_\nu(z)$ and $Y_\nu(z)$ are Bessel and Neumann functions respectively. Substituting the ansatz (A2) and (A3) into (A1) one obtains the following recurrence relation:

$$\left[(2n + \nu)^2 - a\right] c_n + q(c_{n-1} + c_{n+1}) = 0, \qquad (A4)$$

which can be solved in terms of continued fractions. To this end we introduce $h_n^+ = c_n/c_{n-1}$ and $h_n^- = c_{-n}/c_{-n+1}$ for $n > 0$, which substituted into (A4) gives the continued fractions

$$h_n^+ = -\frac{q}{qh_{n+1}^+ + d_n}, \qquad h_n^- = -\frac{q}{qh_{n+1}^- + d_{-n}}, \quad (A5)$$

with $d_n = (2n + \nu)^2 - a$. Characteristic exponent has to be determined from Eq. (A4) for $n = 0$ expressed in terms of h_1^- and h_1^+. In practice, to find numerical values of the coefficients c_n we set $h_m^+ = 0$ and $h_m^- = 0$ for some, sufficiently large m and calculate h_n^+ and h_n^- up to $n = 1$. using (A5).

APPENDIX B: ASYMPTOTIC EXPANSIONS FOR LARGE ARGUMENTS

Asymptotic behavior of $M_\nu(z)$ and $T_\nu(z)$ for large z follows immediately from asymptotic expansions of Bessel functions for large arguments [50]

$$M_\nu(z) \overset{z\to\infty}{\longrightarrow} \sqrt{\frac{2}{\pi}}\frac{e^{-z/2}}{q^{1/4}} s_\nu \cos\left(e^z\sqrt{q} - \frac{\pi}{2}\nu - \frac{\pi}{4}\right) \quad (B1)$$

$$T_\nu(z) \overset{z\to\infty}{\longrightarrow} \sqrt{\frac{2}{\pi}}\frac{e^{-z/2}}{q^{1/4}} s_\nu \sin\left(e^z\sqrt{q} - \frac{\pi}{2}\nu - \frac{\pi}{4}\right) \quad (B2)$$

where $s_\nu = \sum_{n=-\infty}^{\infty} c_n(\nu)$. To obtain asymptotic behavior for large and negative z it is necessary to connect solutions $M_\nu(z)$ and $T_\nu(z)$, with another pair of solution $M_\nu(-z)$ and $T_\nu(-z)$ across $z = 0$ [48]. In this way one obtains [25]

$$M_\nu(z) \overset{z\to-\infty}{\longrightarrow} \sqrt{\frac{2}{\pi}}\frac{e^{z/2}}{q^{1/4}} ms_\nu \cos\left(\sqrt{q}e^{-z} + \frac{\pi}{2}\nu - \frac{\pi}{4}\right) \quad (B3)$$

$$T_\nu(z) \overset{z\to-\infty}{\longrightarrow} -\sqrt{\frac{2}{\pi}}\frac{e^{z/2}}{q^{1/4}}\frac{s_\nu}{m}\left[\sin\left(\sqrt{q}e^{-z} + \frac{\pi}{2}\nu - \frac{\pi}{4}\right)\right.$$
$$\left. - \cot\pi\nu(m^2 - 1)\cos\left(\sqrt{q}e^{-z} + \frac{\pi}{2}\nu - \frac{\pi}{4}\right)\right]$$
$$(B4)$$

where $m = \lim_{z\to 0^+} M_\nu(z)/M_{-\nu}(z)$. To evaluate m numerically, we rather avoid using formula (A2), where

summation over n converges very slowly for $z \to 0$. An alternative approach is to use a different representation for the solutions of the Mathieu's equation [49]

$$W_\nu(z) = \sum_{n=-\infty}^{\infty} c_n(\nu) e^{2n+\nu}, \qquad (B5)$$

where $c_n(\nu)$ are the same coefficients as used in definition of $M_\nu(z)$ and $T_\nu(z)$. One can show that $W_\nu(z)$ differs from $M_\nu(z)$ only by some constant prefactor. We utilize this fact calculating the prefactor at some moderate values of the argument ($z \sim 1$), and then evaluate m using the function $W_\nu(z)$, that has well defined behavior at $z \to 0$.

Finally the radial wave function $\Psi_l(r)$ for partial wave l can be written as linear combination of $M_\nu(z)$ and $T_\nu(z)$

$$\Psi_l(r) = \sin(\phi_l + \tfrac{\pi}{2}\nu + \tfrac{\pi}{4})\sqrt{\frac{R^*}{r}}M_\nu\left(\ln\frac{\sqrt{R^*}}{\sqrt{k}r}\right)$$
$$+ \cos(\phi_l + \tfrac{\pi}{2}\nu + \tfrac{\pi}{4})\sqrt{\frac{R^*}{r}}T_\nu\left(\ln\frac{\sqrt{R^*}}{\sqrt{k}r}\right), \quad (B6)$$

where ϕ_l is a parameter which appear in the small r expansion (6). Now, the behavior of $\Psi(r)$ at small and large distance described by Eqs. (6)-(9), can be readily obtained from asymptotic expansions (B1)-(B4).

APPENDIX C: EXPANSIONS FOR SMALL ENERGIES

Behavior of the parameters m and ν at small energies is given by the following series expansions [61]

$$\nu(q) = l + \tfrac{1}{2} - \frac{q^2}{4(l-\tfrac{1}{2})(l+\tfrac{1}{2})(l+\tfrac{3}{2})} + O(q^4), \quad (C1)$$

and

$$m(q) = \left(\frac{q}{4}\right)^{l+\tfrac{1}{2}} \frac{\Gamma(\tfrac{1}{2}-l)}{\Gamma(\tfrac{3}{2}+l)} + O(q^{l+5/2}), \qquad (C2)$$

where $\psi(x)$ denotes the digamma function [50]. To obtain the above formulas, one can in fact solve the recurrence relation (A4) keeping only the lowest-order terms c_0, c_{-1} and c_1.

[1] G. J. Schulz, Phys. Rev. **125**, 229 (1962).
[2] M. J. W. Boness and G. J. Schulz, Phys. Rev. A **9**, 1969 (1974).
[3] G. J. Schulz, Phys. Rev. Lett. **10**, 104 (1963).
[4] G. J. Schulz, Rev. Mod. Phys. **45**, 378 (1973).
[5] S. J. Buckman and C. W. Clark, Rev. Mod. Phys. **66**, 539 (1994).
[6] Cz. Szmytkowski, K. Maciąg, G.Karwasz, Physica Scripta **54**, 271 (1996).
[7] W. Sun, M. A. Morrison, M. A. Isaacs, W. K. Trail, D. T. Alle, R. J. Gulley, M. J. Brennan and S. J. Buckman, Phys. Rev. A. **52**, 1229 (1995).
[8] R. E. Kennerly, Phys.Rev.A **21** 1876 (1980).
[9] Cz. Szmytkowski, A. Zecca, G. Karwasz, S. Oss, K. Maciąg, B. Marinkoviç, R. S. Brusa, and R. Grisenti, J. Phys. B **20**, 5817 (1987).
[10] C. K. Kwan, Y.-F Hsieh, W. E. Kauppila, S. J. Smith, T. S. Stein, and M. N. Uddin, Phys. Rev. Lett. **52**, 1417 (1984).
[11] G. P. Karwasz , R. S. Brusa, A. Zecca, Rev. Nuovo Cim. **24**, 1 (2001).
[12] J. Ferch, C. Masche and W. Raith, J. Phys. B **14**, L97 (1981).
[13] C. R. Claydon, G. A. Segal, and H. S. Taylor, J. Chem. Phys. **52**, 3387 (1970).
[14] M. A. Morrison, N. F. Lane, and L. A. Collins, Phys. Rev. A **15**, 2186 (1977).
[15] L. A. Collins and M. A. Morrison, Phys. Rev A **25**, 1764 (1982).
[16] M. A. Morrison, Phys. Rev. A **25**, 1445 (1982).
[17] M. Allan, Phys. Rev. Lett. **87** 033201 (2001).
[18] A. K. Kazansky and L. Y. Sergeeva, J. Phys. B **27**, 3217 (1994).
[19] T. N. Rescigno, W. A. Isaacs, A. E. Orel, H.-D. Meyer, and C. W. McCurdy, Phys. Rev. A **65**, 032716 (2002).
[20] T. N. Rescigno, D. A. Byrum, W. A. Isaacs, and C.W. McCurdy, Phys. Rev. A **60**, 2186 (1999).
[21] S. Mazevet, M. A. Morrison, L. A. Morgan and R. B. Nesbet, Phys. Rev. A **64**, 040701(R)
[22] L. A. Morgan, Phys. Rev. Lett. 80 (1998) 1873.
[23] H. Estrada and W. Domcke, J. Phys. B **18**, 4469 (1985).
[24] M. Takekawa and Y. Itikawa, J. Phys. B **29** 4227 (1996).
[25] Z. Idziaszek, G. Karwasz, Phys. Rev. A **73** 064701 (2006).
[26] T. F. O'Malley, L. Spruch, L. Rosenberg, J. Math. Phys. **2**, 491 (1961).
[27] M. A. Morrison, W. Sun, W. A. Isaacs, and W. K. Trail, Phys. Rev. A **55**, 2786 (1997).
[28] H. P. Saha, Phys. Rev. A **39**, 5048 (1989).
[29] G. N. Haddad and T. F. O'Malley, Austr. J. Phys. **35** 35 (1982)
[30] T. Sasakawa and J. Horáĉek, J. Phys. B **15**, L169 (1982).
[31] F. A. Gianturco and K. Willner, Phys. Rev. A **75**, 062714 (2007)
[32] I. I. Fabrikant, H. Hotop, and M. Allan, Phys. Rev. A **71**, 22712 (2005).
[33] I. I. Fabrikant, J. Phys. B: At. Mol. Phys. **16**, 1269 (1983).
[34] W. Vanroose, C. W. McCurdy, and T. N. Rescigno, Phys. Rev. A **68**, 052713 (2003).
[35] J. Ferch, B. Granitza and W. Raith, J. Phys. B. **18**, L445-L450 (1985).
[36] A. Mann and F. Linder, J. Phys. B **25**, 533 (1992).

[37] G. P. Karwasz, A. Karbowski, Z. Idziaszek, R. S. Brusa, Nucl. Instr. and Meth. B, **266**, 471 (2008).

[38] P.A. Macri and R. O. Barrachina, Phys. Rev. A **65**, 062718 (2002).

[39] P.A. Macri and R. O. Barrachina, Nucl. Instr. Methods B **205**, 543 (2003).

[40] S. J. Buckman and J. Mitroy, J. Phys. B **22**, 1365 (1989).

[41] H. R. Sadeghpour, J. L. Bohn, M. J. Cavagnero, B. D. Esry, I. I. Fabrikant, J. H. Macek, and A. R. P. Rau, J. Phys. B **33** R93 (2000).

[42] S. Watanabe, Ch. H. Greene, Phys. Rev. A **22**, 158 (1980).

[43] I. I. Fabrikant, Opt. Spektr. **53**, 223 (1982).

[44] G. P. Karwasz, A. Zecca, R. S. Brusa, *Electron Scattering with Molecules*, in Landolt-Börstein New Series, Volume I/17, Photon and Electron Interaction, with Atoms, Molecules and Ions (Springer-Verlag, Berlin, Heidelberg, 2003), p. 6.1-6.51.

[45] E. Czuchaj, J. Sienkiewicz, and W. Miklaszewski, Chem. Phys. **116**, 69 (1987).

[46] F. A. Gianturco and P. Paioletti, Phys. Rev. A **55** (1997) 3491.

[47] E. Vogt, and G.H. Wannier, Phys Rev. **95**, 1190 (1954).

[48] R.M. Spector, J. Math. Phys. **5**, 1185 (1964).

[49] A. Erdélyi *Higher transcendental functions, Vol. III* (McGraw-Hill, New York, 1955).

[50] M. Abramowitz, I.A. Stegun *Handbook of Mathematical Functions* (Dover, New York, 1972).

[51] T.N. Olney, N.M. Cann, G. Cooper, and C.E. Brion, Chem. Phys. **223**, 59 (1997).

[52] M. Allan, J. Phys. B: At. Mol. Phys. **35**, L387 (2002).

[53] U. Fano, Phys. Rev. **124**, 1866 (1961).

[54] A. Bianconi, AIP Conference Proceedings (2002) XIX Int. Conf. Roma, June 24-28, 2002, arXiv: cond-mat/0211452.

[55] M. Allan, J. Phys. B: At. Mol. Phys. **38**, 3655 (2005).

[56] I. I. Fabrikant, J. Phys. B: At. Mol. Phys. **17**, 4223 (1984).

[57] N.F. Mott and H.S.W. Massey, *Theory of Atomic Collisions*

[58] D.P. Dewangan, and H.R.J. Walters, J. Phys. B: Atom. Molec. Phys. **10**, 637 (1977).

[59] G. P. Karwasz, D. Pliszka, A. Zecca, R. S. Brusa, Nucl. Instr. Meth. B **250**, 666 (2005); G. P. Karwasz, R. S. Brusa, D. Pliszka, Nucl. Instr. Meth. B **251**, 520 (2006).

[60] G. Ramanan and G. R. Freeman, J. Chem. Phys. **93**, 3120 (1990).

[61] J. Meixner, F.W. Schafke *Mathieusche Funktionen und Spharoid Funktionen* (Springer, Berlin, 1954).